PHYSICAL REVIEW C
NUCLEAR PHYSICS

THIRD SERIES, VOLUME 31, NUMBER 5 MAY 1985

Capture of polarized protons by ^{12}C and the interference of compound and direct reaction mechanisms near $E_p = 1.7$ MeV

J. C. Brown,* R. G. Seyler, T. L. Tsin,† and S. L. Blatt
Department of Physics, The Ohio State University, Columbus, Ohio 43210
(Received 22 October 1984)

We have measured the reaction $^{12}C(\vec{p},\gamma_0)^{13}N$ in the energy region of the $E_p = 1.7$ MeV resonance and applied R-matrix theory to its analysis. We used the strong interaction form of the theory where the wave function in the internal region is represented entirely in terms of compound nucleus formation. In order to account fully for the data, an extranuclear direct capture background was found to be necessary, but no internal background was needed.

INTRODUCTION

The direct-capture mechanism has been known for many years to be an important feature of radiative capture reactions. However, when strong resonances dominate the cross section, direct capture is often ignored. Reactions which are of astrophysical importance are ordinarily studied at energies as low as practical considerations permit, and the cross sections are then extrapolated to the still-lower energy region of interest. In such cases, both resonances and any direct-capture components must be taken into account properly, or large errors in extrapolation will occur. It is therefore important to have as much information as possible to bring to bear on these reactions.

In the present work, we have studied the reaction $^{12}C(\vec{p},\gamma)^{13}N$, and show that measurements of analyzing powers in this radiative capture reaction help to pin down the direct-capture component through its interference with the known strong resonances. It is hoped that this result will encourage similar measurements on other (p,γ) reactions, using this additional information to confirm present knowledge or to discover additional significant contributions to the cross sections at the very low energies of interest for understanding stellar processes.

The present measurements employed an energy-dispersive "thick target" method,[1] previously applied only for yield curve measurements, to measure the detailed energy dependence of the reaction's analyzing power over an entire resonance in a single accelerator setting.[2] The method, applicable to many similar reactions, reduces dependence on accelerator resolution and stability, substituting instead the performance characteristics of a Ge(Li) detector.

The theoretical analysis was carried out in the framework of R-matrix formalism, with careful attention to the details needed for proper inclusion of the photon channel. Earlier parametrizations[3,4] of the $^{12}C(p,\gamma)^{13}N$ reaction, which either ignored the direct component or did not utilize sufficient angular information, are found to be inadequate to describe the measured analyzing powers, but our analysis satisfactorily explains all of the available data.

EXPERIMENTAL PROCEDURE

Measurements were made over the 1.7 MeV resonance in $^{12}C(p,\gamma_0)^{13}N$, utilizing a 49.5 cm^3 active-volume closed-end cylindrical Ge(Li) detector (Canberra) mounted on an arm free to rotate in a horizontal plane about the target. The beam of polarized protons was obtained utilizing the Ohio State University ion source ORION (Ref. 5) mounted in the terminal of our HVEC "super-CN" Van de Graaff accelerator. Beam current was monitored both by direct current integration and the use of a 2.5×2.5 cm NaI(Tl) detector mounted just below the beam line, to observe gamma rays from the target at $\theta_\gamma \approx 180°$. The polarization orientation of the proton beam was reversed by changing the ionizer field in the source; the magnitude and sign of the beam polarization p_y were periodically checked with p-^{4}He scattering in a chamber designed to perform a "proper flip," reversing the roles of left and right detectors.

Data for cross-section angular distribution measurements were recorded at $-90°$, $-60°$, $-30°$, $+110°$, and $+120°$, where "+" ("−") indicates that the angle was to the right (left) of the proton beam. Analyzing power measurements, taken with lower beam currents, were made at $-90°$, $-30°$, and $-112.5°$. For the latter runs, a regular sequence of spin-up and spin-down spectra was recorded.

Thick-target spectra were taken using reactor-grade graphite targets. Since the 1.7 MeV resonance is consider-

ably broader than the intrinsic resolution of the Ge(Li) detector, and since the energy of the outgoing gamma rays in a (p,γ) reaction is a linear function of the proton energy, the observed gamma-ray spectra trace out the resonance shape as the protons slow down within the target. Figure 1 shows the high-energy portion of ionizer plus/minus spectra (corresponding to the two orientations of proton spin) during the accumulation of data at $-90°$. Figure 2 shows, on an expanded scale, a sequence of graphs showing how spectra are transformed into plots of cross section versus energy. A small flat background, visible above the 1.7 MeV resonance peak in Fig. 1, is first subtracted and a correction is made for the Doppler shift, which varies with angle and therefore alters the relationship of gamma-ray spectrum channel vs E_p from angle to angle. A thin-target line shape [shown in Fig. 2(b)] is then used to strip the corrected spectrum, and a correction for the stopping power of carbon as a function of proton energy is applied. The final "spectrum" is an accurate representation of gamma-ray yield vs E_p for the particular angle and beam polarization being run.

Angular distributions were extracted from these yield curves in ~ 18 keV bites. Corrections for detector efficiency and solid angle were applied, and Legendre polynomial fits were made in the usual way. The results are in good agreement with those of Young *et al.*[3] Since that experiment measured the unpolarized angular dependence in more detail than the present one, as well as covering a wider energy range, those data were actually used below, both for determining reaction parameters and for the non-polarization-dependent coefficients needed in computing our analyzing power coefficients.

For the analyzing power runs, asymmetries

$$A = p_y A_y = \frac{N_u - N_D}{N_u + N_D}$$

were determined utilizing the gamma-ray yields taken with spin up (N_u) and those with spin down (N_D). A small difference in the magnitude of "ionizer +" polarization (~ 0.71) and "ionizer −" polarization (~ 0.69) was taken into account. Figure 3 shows the analyzing powers A_y obtained in this experiment.

THEORY

We have chosen to analyze the $^{12}C(p,\gamma_0)^{13}N$ analyzing power data in terms of R-matrix theory,[6] in which a nearly model independent direct capture contribution to radiative capture reactions is realized as a result of integration in the entrance channel. In the approach followed, internal and external transitions arise in the capture reaction problem on an equal footing, as having the same origin. Consequently, no phenomenology is required in the formal description of these reactions; in particular, no phase ambiguity between extranuclear direct capture and other capture mechanisms is involved. The spatial integral involving the initial ψ_i and final ψ_f wave functions and the electromagnetic operator $\sqrt{2\pi\rho}/\hbar H_{\text{int}}$ that produces the radiative capture collision matrix integral, i.e.,

$$I_c = -\sqrt{2\pi\rho}/\hbar \int d\tau \psi_f H_{\text{int}} \psi_i \ , \tag{1}$$

is conveniently split into a sum of two integrals, one involving integration over a channel dependent internal region ($r \leq a_c$) and the other over an external region ($r \geq a_c$), using wave functions and operators appropriate for these regions.

The initial wave function for unit incident particle flux

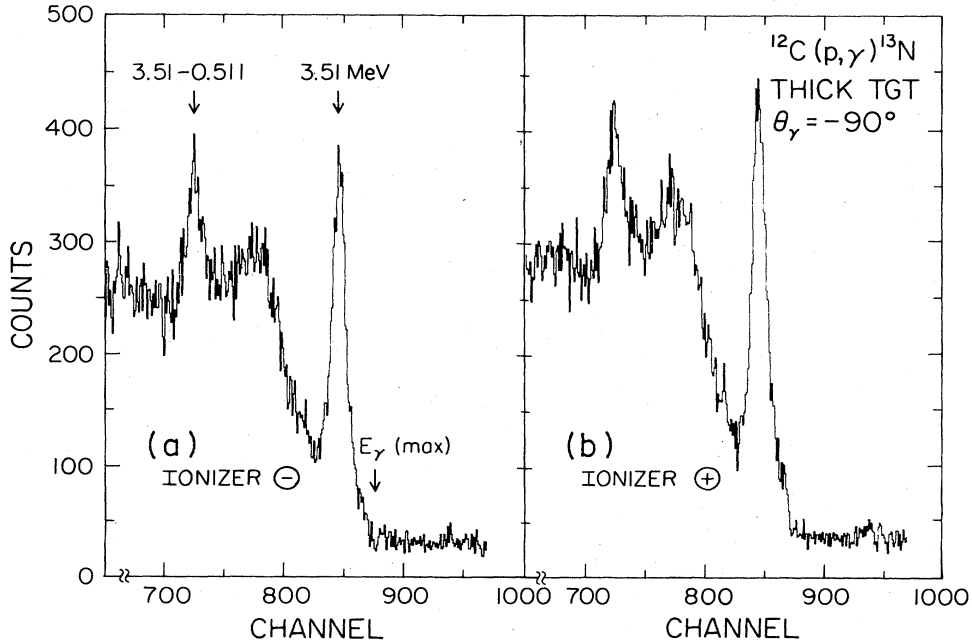

FIG. 1. High energy of ionizer − and ionizer + thick-target spectra for $^{12}C(\vec{p},\gamma_0)^{13}N$ at $\theta_\gamma = -90°$. The two ionizer polarities produce beam polarizations up and down with respect to the reaction plane. Visible features include the energy-dispersed full energy and one-escape peaks, the Compton edge between these, and a flat background due primarily to cosmic rays. A small discontinuity at about channel 870 marks the maximum energy γ ray produced by the incoming 1.8 MeV proton beam.

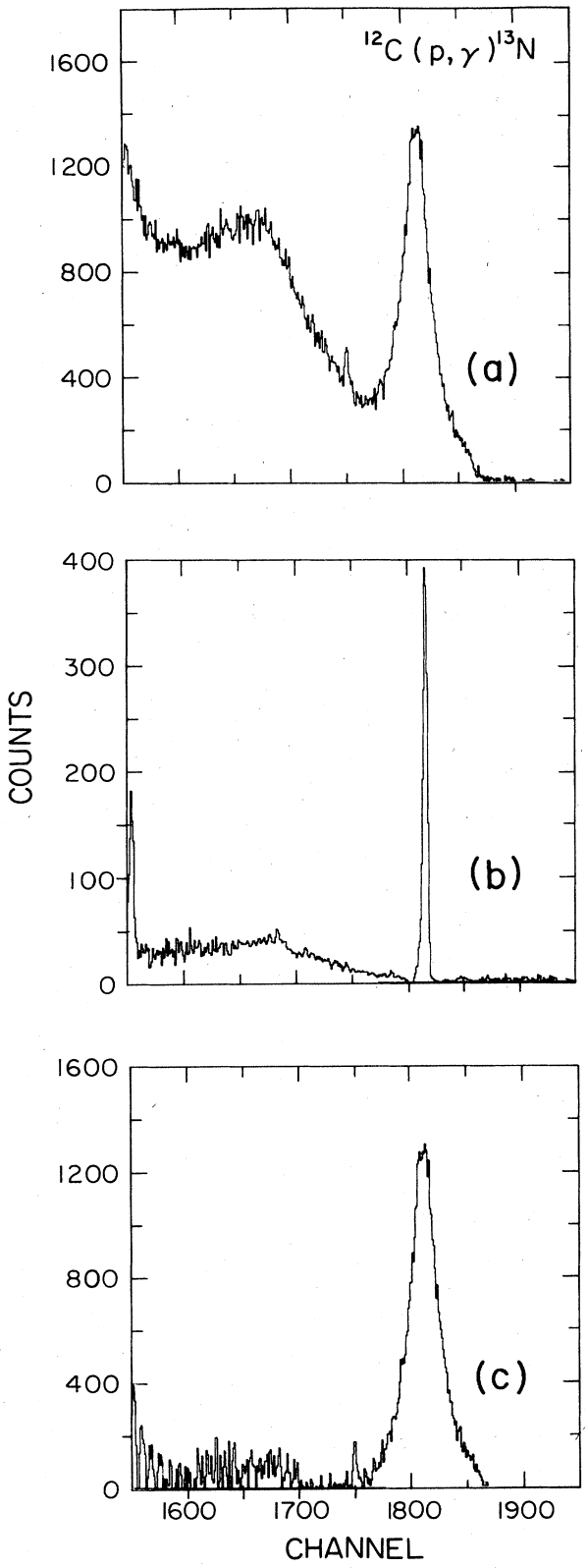

FIG. 2. Sequence showing reduction of experimental spectra to yield vs E_p. (a) Background subtracted, Doppler shift corrected; (b) thin-target line shape to deconvolute data; (c) resulting yield curve. The small peak near channel 1750 is from ^{13}C in the target, and was excluded from the data analysis.

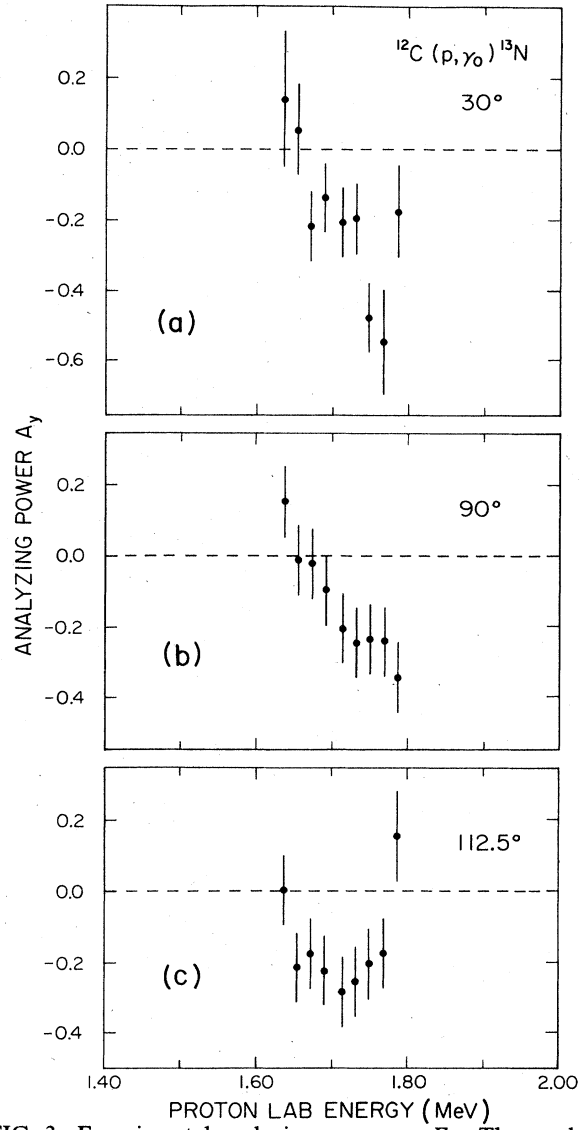

FIG. 3. Experimental analyzing powers vs E_p. These values were used, together with the A_k's of Fig. 5, to determine the B_J's plotted in Fig. 6.

in the channel $i(\alpha ls)$ is

$$\psi_i^{JM} = -i\sqrt{\hbar} e^{i(\omega_i-\phi_i)} \sum_{\lambda,\mu} A_{\lambda,\mu} \Gamma_{\mu i}^{1/2} \chi_\lambda^{JM}, \quad (r \leq a_c),$$

$$= \sum_{m,\nu,\nu'} \frac{i\sqrt{\pi}}{\sqrt{v}\, rk} (lm,s\nu \mid JM) i^l Y_l^m \hat{l} \times \psi_{\alpha s\nu}(I_{\alpha l} - e^{2i\delta_i^J} O_{\alpha l})(l0,s\nu' \mid JM), \quad (r \geq a_c), \tag{2}$$

where, following the notation of Ref. 6, ω_i is the Coulomb phase shift, ϕ_i is the hard sphere phase shift, $A_{\lambda,\mu}$ is the level matrix, $\Gamma_{\mu i}$ is the partial width of the proper level μ in the channel i, and χ_λ^{JM} is the proper function of the level λ. The initial wave function in the external region has been specialized to include only elastic scattering.

The function $\psi_{\alpha s\nu}$ is the channel spin wave function, v is the relative velocity of the pair α, k is the wave number, I_{al} is related to the incoming wave Coulomb function, i.e.,

$$I_{al}=(G_{al}-iF_{al})e^{i\omega_{al}} , \tag{3}$$

and O_{al} is the complex conjugate of I_{al}. δ_l^J is the phase shift.

In the external region, the final bound state wave function for total spin B and projection M_B is

$$\psi_f^{BM_B}=\sum_{\substack{m\nu\\ l_b s}}(l_b m,s\nu\,|\,BM_B)N_b^{1/2}\frac{2^{1/2}\theta_{l_b s}}{\sqrt{a_{l_b s}}}i^{l_b}Y_{l_b}^m$$

$$\times\psi_{\alpha s\nu}W_{l_b}(r)/[rW_{l_b}(a_{l_b s})] , \tag{4}$$

where $W_{l_b}(r)$ is the Whittaker function, and $\theta_{l_b s}$ is the dimensionless reduced partial width amplitude of the bound state. The factor N_b is determined by the normalization condition on the bound state

$$\int|\psi_f^{BM_B}|^2 d\tau=1 , \tag{5}$$

and is given by

$$N_b=\left\{1+\sum_{c^-}\frac{2\theta_{c^-}^2}{a_{c^-}}\int_{a_{c^-}}^{\infty}dr\left[\frac{w_{c^-}(r)}{w_{c^-}(a_{c^-})}\right]^2\right\}^{-1} . \tag{6}$$

From Eqs. (1), (2), and (4) the extranuclear part of the collision matrix element for an electric dipole transition from an initial continuum state characterized by channel spin s, relative orbital angular momentum l, reduced mass μ, and wave number k to a final bound state of spin B and relative orbital angular momentum l_b with the emission of a photon of wave number k_γ, is

$$U_{E1B,ls}^{J(\text{ext})}=(-)^{l+s-B}N_b^{1/2}\left[\frac{6k_\gamma^3\mu e^2}{\hbar^2 ak}\right]^{1/2}\hat{l}\hat{B}\theta_{l_b s}$$

$$\times(i)^{l-l_b-1}R_{ll_b s}^J(l0,10\,|\,l_b 0)W(JlBl_b;s1) , \tag{7}$$

where

$$R_{ll_b s}^J=\int_a^{\infty}dr\frac{w_{l_b}(r)}{w_{l_b}(a)}\frac{G_1}{k_\gamma}(I_l-l^{2i\delta_{ls}^J}O_l) . \tag{8}$$

The radial part of the electric dipole operator in the external region is

$$G_1=Z_1\left[k_\gamma\frac{m_2}{m}j_0\left[k_\gamma\frac{m_2}{m}\right]-j_1\left[k_\gamma\frac{m_2}{m}\right]\right]$$

$$-Z_2\left[k_\gamma\frac{m_1}{m}j_0\left[k_\gamma\frac{m_1}{m}\right]-j_1\left[k_\gamma\frac{m_1}{m}\right]\right] , \tag{9}$$

where Z_1 (Z_2) is the charge of the projectile (target) in units of the proton charge e, m_1 (m_2) is the mass of the projectile (target), m is the total mass, and the functions j_0 and j_1 are the spherical Bessel functions. In the external region, transitions corresponding to higher order multipoles contribute negligibly for low energy reactions.

The external collision matrix elements are determined to within the (measurable) elastic scattering phase shifts and an energy independent scaling factor $N_b^{1/2}\theta_{l_b s}$. The total collision matrix for electric dipole transitions, i.e.,

$$U_{E1B,ls}^J=N_b^{1/2}ie^{i(\omega_l-\varphi_l)}$$

$$\times\sum_{\lambda,\mu}A_{\lambda,\mu}\Gamma_{\mu,ls}^{1/2}\Gamma_{\lambda f}^{1/2}+U_{E1B,ls}^{J(\text{ext})} , \tag{10}$$

where

$$\Gamma_{\lambda f}^{1/2}=\sqrt{2\pi\rho}\langle\psi_f'^B||H_{\text{int}}||\chi_\lambda^J\rangle ,$$

is then essentially stripped of the contribution corresponding to known external electric dipole transitions. An additional (often overlooked) feature of the introduction of these explicit background terms is that they are tantamount to additional states (J^π), which become particularly apparent in accounting for interference observables such as analyzing powers. In the present application, the resonances are isolated and consequently the internal collision matrix elements reduce to simple Breit-Wigner forms, as will be seen later.

The total (internal plus external) collision matrix element for the radiative capture reaction $A(a,L)B$ is related to the photon scattering amplitude through the relation

$$A_{\epsilon m_B;m_a m_A}=\frac{i\sqrt{\pi}}{k}\sum_{JM}\sum_{\substack{ls\nu\\ Lp\Lambda}}\frac{\hat{l}\hat{L}}{\sqrt{8\pi}}\epsilon^p D_{\Lambda\epsilon}^{L*}(\hat{\mathbf{k}}_\gamma)(am_a,Am_A\,|\,s\nu)(L\Lambda,Bm_B\,|\,JM)(l0,s\nu\,|\,JM)U_{LpB;ls}^J \tag{11}$$

where ϵ is the photon's helicity, p represents the mode of the outgoing radiation [$p=1$ (magnetic), $p=2$ (electric)], and $D_{\Lambda\epsilon}^L(\hat{\mathbf{k}})$ is an element of the rotation matrix. The remaining spin projections are on the incident beam's direction.

The cross section for a polarized incident beam of spin $\frac{1}{2}$ particles in terms of the photon scattering amplitude (matrix) is

$$\frac{d\sigma}{d\Omega}=\frac{1}{\hat{a}^2\hat{A}^2}[\text{Tr}(AA^\dagger)+p_y\text{Tr}(A\sigma_y A^\dagger)] . \tag{12}$$

Using Eq. (11), Eq. (12) may be expressed in terms of the associated Legendre polynomials, as in Ref. 7,

$$\frac{d\sigma}{d\Omega}=\frac{(\lambda\!\!\!^{-}/2)^2}{\hat{a}^2\hat{A}^2}\left[\sum_{k=0}a_k P_k+p_y\sum_{k=1}b_k P_k^1\right] . \tag{13}$$

The Legendre coefficients, a_k and b_k, are given by Eqs. (20) and (21) in Ref. 7, with the exception that in place of the general reduced transition matrix element $\langle pL(B)J\pi||R||l(a\Lambda)sJ\pi\rangle$, we have the well-defined total collision matrix element $U^J_{LpB,ls}$, representing gamma transitions in the internal and external regions.

RESULTS AND DISCUSSION

Application of the direct capture formalism is particularly straightforward in the p + ^{12}C radiative capture reaction for bombarding energies in the vicinity of 1.70 MeV. Three isolated resonance internal collision matrix elements contribute,

$$U_0^{1/2^+}(E1),\ U_1^{3/2^-}(M1),\ U_1^{3/2^-}(E2)\ .$$

The abbreviated notation represents the formation of the $\frac{1}{2}^+$ level (superscript) by the capture of s wave protons (subscript) which decays by $E1$ radiation to the $\frac{1}{2}^-$ ^{13}N ground state (Fig. 4). The $\frac{3}{2}^-$ level is formed by the capture of p wave protons and decays by either $M1$ or $E2$ radiation to the ^{13}N ground state. Resonant gamma rays from the $E_x=3.547$ MeV level ($J^\pi=\frac{5}{2}^+$) have not been observed, and therefore this level has been excluded in the final analysis after determining that the interference between this level and the two lower levels at $E_x=2.366$ MeV and $E_x=3.512$ MeV could not account for the differential cross section and analyzing power angular distributions simultaneously. This preliminary analysis included the use of $\frac{1}{2}^+$, $\frac{3}{2}^-$, and $\frac{5}{2}^+$ background contributions. The next resonant state above the $E_x=3.547$ MeV level occurs at $E_x=6.382$ MeV ($J^\pi=\frac{5}{2}^+$), and, from the preliminary analysis, does not influence the observed capture reaction data for $E_x<4.0$ MeV.

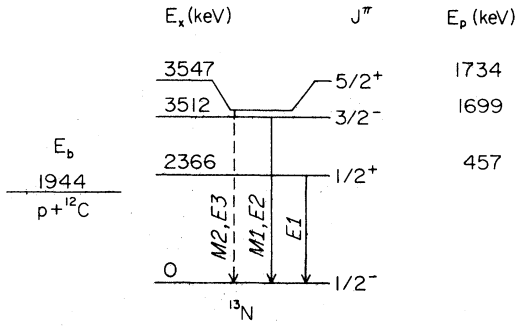

FIG. 4. Energy level diagram for ^{13}N.

The two external collision matrix elements which contribute (only $E1$ elements need be considered) are

$$U_0^{1/2^+}(E1),\ U_2^{3/2^+}(E1)\ .$$

The second of these represents the d wave direct capture to the $l_b=1$ final bound state and corresponds to a new collision matrix element ($\frac{3}{2}^+E1$) relative to an analysis based on the resonance levels and their associated backgrounds as the only source of collision matrix elements ($\frac{1}{2}^+E1, \frac{3}{2}^-M1, \frac{3}{2}^-E2$). Strictly speaking, there is nothing unusual in this approach to including background since all possible j^π background contributions are admissible. The procedure followed here simply focuses on a particular background, which may be expected to dominate.

The ^{12}C(p,γ_0)^{13}N a_0, a_1, a_2, and b_1 coefficients are, from Eq. (13),

$$a_0=2[\,|U_0^{1/2^+}(E1)|^2+2|U_1^{3/2^-}(M1)|^2+2|U_1^{3/2^-}(E2)|^2+2|U_2^{3/2^+}(E1)|^2]\ , \tag{14}$$

$$a_1=2\left\{2\,\mathrm{Re}[U_0^{1/2^+}(E1)U_1^{3/2^-}(M1)^*]+2\sqrt{3}\,\mathrm{Re}[U_0^{1/2^+}(E1)\times U_1^{3/2^-}(E2)^*]\right.$$
$$\left.+\frac{2\sqrt{3}}{5}\mathrm{Re}[U_1^{3/2^-}(E2)U_2^{3/2^+}(E1)^*]-2\,\mathrm{Re}[U_1^{3/2^-}(M1)\times U_2^{3/2^+}(E1)^*]\right\}\ , \tag{15}$$

$$a_2=2\{|U_1^{3/2^-}(E2)|^2-|U_1^{3/2^-}(M1)|^2-|U_2^{3/2^+}(E1)|^2-2\,\mathrm{Re}[U_0^{1/2^+}(E1)U_2^{3/2^+}(E1)^*]$$
$$+2\sqrt{3}\,\mathrm{Re}[U_1^{3/2^-}(M1)U_1^{3/2^-}(E2)^*]\}\ , \tag{16}$$

and

$$b_1=2\left\{\sqrt{3}\,\mathrm{Re}[iU_1^{3/2^-}(E2)U_0^{1/2^+}(E1)^*]+\mathrm{Re}[iU_1^{3/2^-}(M1)U_0^{1/2^+}(E1)^*]\right.$$
$$\left.+4\,\mathrm{Re}[iU_2^{3/2^+}(E1)U_1^{3/2^-}(M1)^*]+\frac{4\sqrt{3}}{5}\mathrm{Re}[iU_1^{3/2^-}(E2)U_2^{3/2^+}(E1)^*]\right\}\ . \tag{17}$$

The coefficients in Eqs. (14)—(17) are not model dependent. The coefficients in the b_1 expression, Eq. (17), agree with Ref. 8 as amended by Ref. 9. The collision matrix elements in Eqs. (14)—(17) are here taken to have the following forms:

$$U_0^{1/2^+}(E1)=N_b^{1/2}\left[X(1)U_0'^{1/2^+}(\text{ext})+\frac{ie^{i(\omega_0-\varphi_0)}\sqrt{2P_0}\gamma_0 X(2)(E_\gamma/E_R)^{3/2}}{E_R(\frac{1}{2}^+)-S_0^0\gamma_0^2-E-iP_0\gamma_0^2}\right], \tag{18}$$

$$U_1^{3/2^-}(M1)=N_b^{1/2}\left\{\frac{ie^{(\omega_1-\varphi_1)}\sqrt{2P_1}[\gamma_1+X(6)]X(4)[E_\gamma/(E_R(\frac{3}{2}^-)+X(3))]^{3/2}}{E_R(\frac{3}{2}^-)+X(3)-S_1^0(\gamma_1+X(6))^2-E-iP_1(\gamma_1+X(6))^2}\right\}, \tag{19}$$

$$U_1^{3/2^-}(E2)=\frac{X(5)}{X(4)}[E_\gamma/(E_R(\tfrac{3}{2}^-)+X(3))]U_1^{3/2^-}(M1), \tag{20}$$

and

$$U_2^{3/2^+}(E1)=N_b^{1/2}X(1)U_2'^{3/2^+}(\text{ext}), \tag{21}$$

where U' is the U(ext) of Eq. (7) except for the omission of the scaling factor $N_b^{1/2}\theta_{l_b s}$,

$$N_b=\left\{1+\frac{2X(1)^2}{a}\int_a^\infty dr\left[\frac{W_1(r)}{W_1(a)}\right]^2\right\}^{-1},$$

and $X(1)$ through $X(6)$ are parameters given in Table I. In Eq. (18), the external collision matrix element $U_0'^{1/2^+}$(ext) adds to a dominant internal element (arising from the $\frac{1}{2}^+$ resonance at $E_x=2.366$ MeV) and thus has little effect on the overall interference pattern in the vicinity of $E_x=3.5$ MeV. However, the $U_2'^{3/2^+}$(ext) external collision matrix element of Eq. (21) has no corresponding internal collision matrix element and thus is the source of a sizable analyzing power owing to its interference with the $M1$ and $E2$ transitions from the $\frac{3}{2}^-$ level, as can be seen from Eq. (7).

The six parameters $X(i)$ in Eqs. (18)—(21) were varied in order to minimize the chi-squared function χ^2 composed of the experimental A_0, A_1, and A_2 coefficients of Ref. 3 and the corresponding theoretical quantities, Eqs. (14)—(16) ($A_k=\lambda\!\!\!^{-2}a_k/8$). The results are reported in Table I. The starting parameters in the search reported in Table I were taken from Ref. 3. In these expressions, the sum over the remaining bound channels at $E_b=1.944$ MeV in the normalizing factor N_b [Eq. (6)] and the sum over the negative energy channels at the incident excitation energy in the shift function were neglected. The sum over bound channels at $E_b=1.944$ MeV is expected to be small due to the relatively high separation energies of other negative energy channels (integral over the external region of these tightly bound configurations is small) and due to the large p+^{12}C parentage in the ^{13}N ground state as deduced from stripping and other reactions,[14] and therefore of only negligible influence on the overall normalization factor. The neglect of negative energy channels in the shift function is essentially on the same basis. The percent uncertainty in the last column of Table I was crudely obtained by arbitrarily *doubling* the uncertainty observed in the best fit parameters obtained from χ^2 searches performed with different sets of parameter values. The 30% uncertainties in $X(3)$ and $X(6)$ are misleadingly large since these parameters represent deviations of the values of physical quantities from their earlier found values. For example, $X(3)=0.2\pm0.06$ keV means that the $\frac{3}{2}^-$ resonance energy is 0.2 keV greater than the value of Ref. 10, which implies that this nearly 1700 keV (lab) resonance energy has a very small percentage uncertainty. Similarly, the deviation parameter $X(6)$ corresponds to a physical quantity $\gamma_p(\frac{3}{2}^-)$, the proton reduced width amplitude for the $\frac{3}{2}^-$ resonance, having the value (0.330 ± 0.008) MeV$^{1/2}$ which involves an uncertainty of only about 2%. The square of the parameter $X(2)$ is the $\frac{1}{2}^+E1$ partial width at resonance. Since the $\frac{1}{2}^+$ state lies outside (below) the energy range of this analysis it should not be surprising that its partial width would be our least accurately determined parameter. A final comment on the parameter uncertainties involves the rather well-determined parameters $X(4)$ and $X(5)$, which, when

TABLE I. Parameters used in χ^2 minimization.

	Initial value	Final value	% Uncertainty
$X(1)$ $\theta_1(\frac{1}{2}^-)$	0	0.41	12
$X(2)$ $[\Gamma_\gamma^R(\frac{1}{2}^+,E1)]^{1/2}$	0.82 eV$^{1/2}$	0.59 eV$^{1/2}$	18
$X(3)$ $\delta E_R(\frac{3}{2}^-)$	0	0.2 keV	30
$X(4)$ $[\Gamma_\gamma^R(\frac{3}{2}^-,E2)]^{1/2}$	−0.077 eV$^{1/2}$	−0.079 eV$^{1/2}$	6
$X(5)$ $[\Gamma_\gamma^R(\frac{3}{2}^-,M1)]^{1/2}$	0.83 eV$^{1/2}$	0.77 eV$^{1/2}$	6
$X(6)$ $\delta\gamma_p(\frac{3}{2}^-)$	0[a]	0.026 MeV$^{1/2}$	30
χ^2	2841	348	

[a]Reference 10: $\gamma_p(\frac{1}{2}^+)=1.26$ MeV$^{1/2}$, $\gamma_p(\frac{3}{2}^-)=0.304$ MeV$^{1/2}$. The initial $\gamma_p(\frac{3}{2}^-)$ gives an observed total width (Ref. 6) $\Gamma^0(\frac{3}{2}^-)=53$ keV (lab) for $a_c=4.77$ fm (Ref. 10). The final $\gamma_p(\frac{3}{2}^-)=0.330$ MeV$^{1/2}$ gives $\Gamma^0(\frac{3}{2}^-)=61$ keV (lab).

squared, are the $\frac{3}{2}^-$ $E2$ and $M1$ partial widths (at resonance), respectively. From Eq. (20) the ratio of the $\frac{3}{2}^-$ $E2$ and $M1$ collision matrix elements is directly proportional to the ratio $X(5)/X(4)$ and it turns out that this ratio is much more accurately determined by the data than is either $X(5)$ or $X(4)$.

Our very limited exploration of the χ^2 surface does not permit us to rule out the presence of other independent solutions (parameter sets). We contented ourselves with the set of Table I since these parameters were reasonably consistent with earlier work and resulted in a good fit to the observables (the square root of the χ^2 per data point had the value of 2.6). This is in keeping with our motivation which has been to demonstrate that the parameter-free external collision matrix formalism could conveniently be employed to satisfactorily describe the data with reasonable parameter values rather than to determine the parameter values or their uncertainties extremely accurately.

The best fit parameters include a dimensionless reduced partial width $\theta^2[=X^2(1)]$ for the p+^{12}C (g.s.) channel in the ^{13}N ground state of 0.17 ± 0.04. Using for the dimensionless single particle (sp) reduced partial width the value[11] $\theta^2_{\rm sp}=0.6$ (good to perhaps 30%) allows one to calculate the value $C^2S=0.29\pm0.14$ for the spectroscopic factor of the p +^{12}C (g.s.) component of the ^{13}N ground state. This value is too low to be in agreement with the Cohen and Kurath[12] shell model prediction of 0.61, but is possibly in reasonable agreement with the experimental value of 0.49 ± 0.15, deduced by Rolfs and Azuma in their (p,γ_0) analysis[4] and the lowest of the range of values 0.5—1.5 deduced from stripping analyses[13] (S would have a maximum value of unity for capture into an empty shell). Turning this argument around, we might accept the recent and definitive stripping analysis results $C^2S=0.48$ of Peterson and Hamill.[13] Then our best fit value of θ^2 would imply $\theta^2_{\rm sp}=0.36$ (with an uncertainty range of ±0.11, assuming a 20% uncertainty in the C^2S value). Although this 0.36 value is 40% lower than the 0.6 value used by Lane[11] for analyzing resonance reactions, he mentions that the 0.6 value is uncertain by perhaps 30% for resonance reactions and points out that in the case of negative energy nucleon channels, as in the present case of the ^{13}N (g.s.), one can expect $\theta^2_{\rm sp}$ to have an even lower value. Therefore we can conclude that our result for θ^2 is completely consistent with C^2S and $\theta^2_{\rm sp}$ values deduced or used by other workers.

The square root of the $E2$ and $M1$ partial width ratio at resonance is -0.102 ± 0.003. The corresponding mixing ratio in Ref. 3 is -0.092 and in Ref. 4 is -0.09 ± 0.02. Using the $\omega\Gamma_\gamma$ value of 1.19 eV (Table I), and a total resonance cross section of 37.5 μb[3] gives a total width Γ (lab) for the 3.51 MeV level of 62 keV, which is in good agreement with the results of previous work.[4] The mixing ratio α_1^2, defined in Ref. 3 as

$$\alpha_1^2=\frac{\Gamma_\gamma^R(\frac{3}{2}^-,M1)}{\Gamma_\gamma^R(\frac{1}{2}^+,E1)}\left[\frac{2.37}{3.51}\right]^3,$$

is given as 0.319. The corresponding mixing ratio in the present work is 0.52, primarily reflecting a smaller γ-ray partial width for the 2.37 MeV level.

The ^{12}C(p,γ_0)^{13}N A_0, A_1, and A_2 coefficients are plotted as a function of incident proton energy in Fig. 5. The open circles are the data of Ref. 3, the dashed line is the Legendre coefficient as calculated with only the external collision matrix elements [$U_0^{1/2^+}(E1)$ and $U_2^{3/2^+}(E1)$], the dotted line is the Legendre coefficient with only the internal collision matrix elements [$U_0^{1/2^+}(E1)$, $U_1^{3/2^-}(M1)$, and $U_1^{3/2^-}(E2)$], and the solid line is the complete Legendre coefficient. The solid line represents the best fit to the data. From Figs. 5(a) and (c), the external direct capture contribution to the A_0 and A_2 coefficients is virtually negligible over the resonance. The A_1 coefficient in Fig. 5(b), however, is considerably altered relative to internal collision matrix contributions. From Eq. (15), the drop through zero in Fig. 5(b) is seen to result from the direct capture $\frac{3}{2}^+$ $E1$ collision matrix element interfering with the dominant $\frac{3}{2}^-$ $M1$ transition.

Even though external contributions were limited to electric dipole transitions, a small A_3 coefficient can arise from interference between the $\frac{3}{2}^-$ ($L=2,p=2,l=1$) resonance and the pseudo $\frac{3}{2}^+$ ($L=1,p=2,l=1$) resonance. The predicted smallness of the A_3 coefficient is consistent with its neglect in the data reduction performed by Young *et al.*[3]

To determine the experimental b_k, our measured analyzing powers for the ^{12}C(p,γ_0) ^{13}N reaction near $E_p=1.70$ MeV (shown earlier in Fig. 3) were multiplied by the differential cross sections determined by the analysis of the data of Ref. 3. The resulting angular distributions of the analyzing power-differential cross section product were then least squares fit with the $m=1$ associated Legendre polynomials of order $k=1$ [Fig. 6(a)] and $k=3$ [Fig. 6(b)], where $B_k=\lambda\!\!\!^{-2}b_k/8$. Terms of order $k=1$ through $k=3$ are expected in this expansion. However, as there are only three experimental points in the analyzing power angular distributions, the $k=2$ coefficient was neglected on the basis that it was the least significant in this energy region, corresponding to interference of background terms. The $k=3$ coefficient, on the other hand, involves interference between the $\frac{3}{2}^-$ resonance and background and is larger.

In Fig. 6, the solid lines are the predictions for B_1 and B_3 resulting from our theoretical fit to only the A_0, A_1, and A_2 coefficients of Ref. 3. The theoretical curves are merely overlaid on the analyzing power data; *the analyzing power data have not been included in the chi-squared minimization program.* The analyzing power data have large relative errors, and, as can be seen by comparison of Figs. 5 and 6, the error in the fit to the B's is no worse than the fit to the A's. So there is little to be gained by including the analyzing power data in the minimization program. It is encouraging to note that the extranuclear direct capture formalism is entirely adequate to account for the ^{12}C(p,γ_0)^{13}N reaction over the energy region of the second resonance. We hasten to point out, however, that whereas in the present study the analyzing power data simply confirmed the prediction based on our analysis of the unpolarized data, this situation is probably atypical. The reason one expects to need the polarized data in addi-

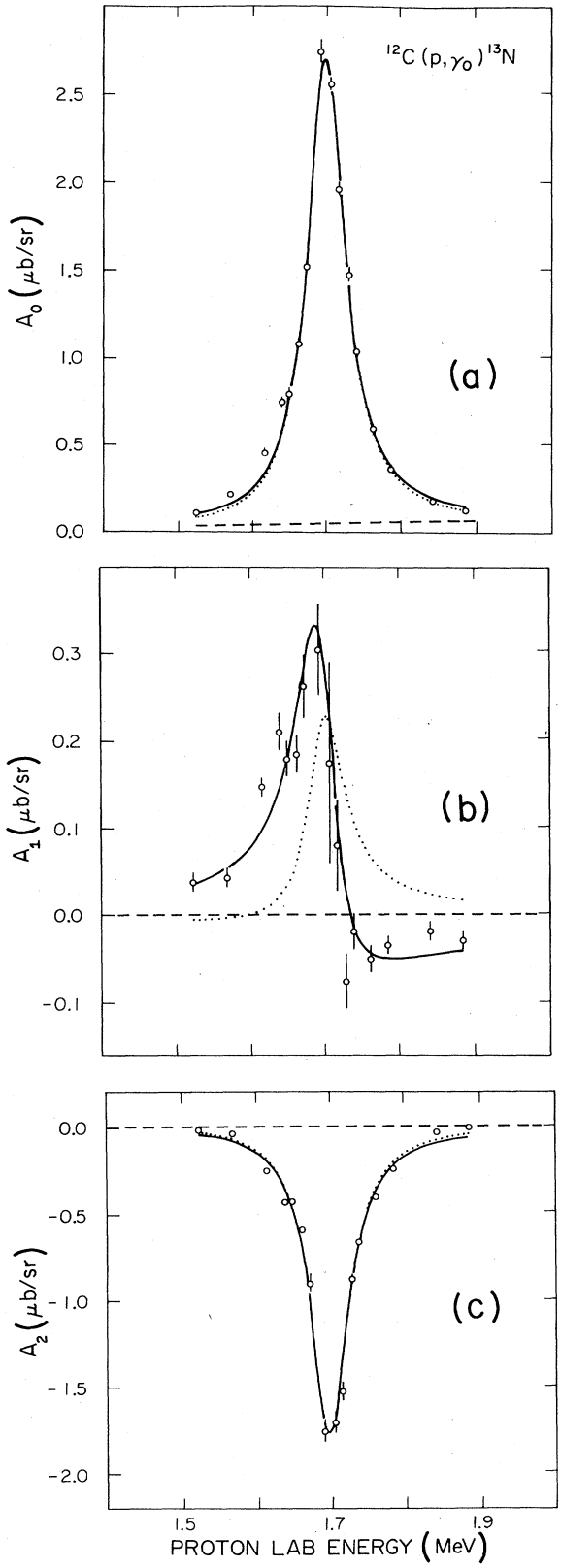

FIG. 5. ^{12}C(p,γ_0)^{13}N angular distribution coefficients vs E_p over the energy region of the 1.70 MeV resonance. (a) A_0; (b) A_1; (c) A_2. The data are taken from Ref. 3. See the text for explanation of the curves.

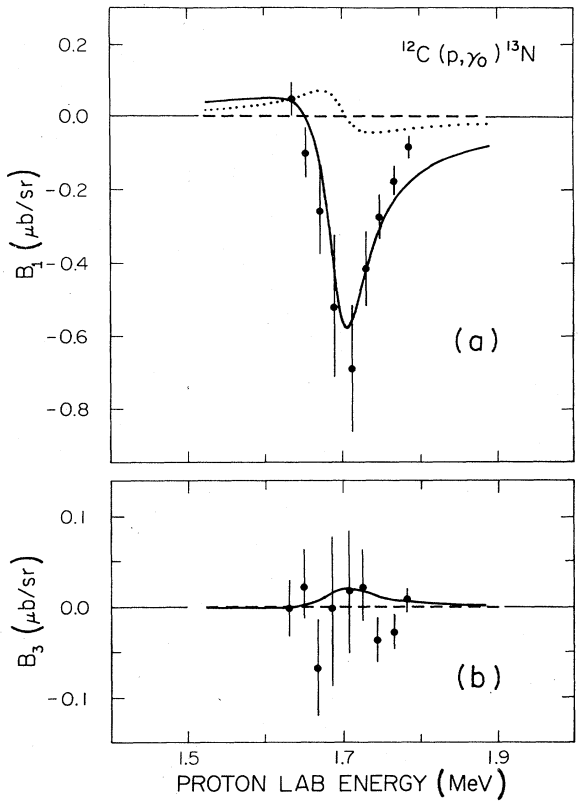

FIG. 6. Analyzing-power x cross-section coefficients vs E_p. Data are derived from those of Figs. 3 and 5. (a) B_1; (b) B_3. Curves are predictions based on the parameters derived from fits to the unpolarized data.

tion to the unpolarized data can be seen by comparing Eq. (15) for a_1 and Eq. (17) for b_1. Both a_1 and b_1 contain only interference contributions (rather than squares of magnitudes of certain matrix elements, as is the case for a_0 or a_2) and are therefore more sensitive to small matrix elements than a_0 or a_2. Furthermore, the same collision matrix pairs occur in both a_1 and b_1 but with two very important differences. First, the various pairs are weighted differently in a_1 than in b_1, and second, a_1 depends on the real part of products like $U_1U_2^*$ which involves the *cosine* of the difference of their phase angles, whereas b_1 depends on $\mathrm{Re}(iU_1U_2^*)$ which involves the *sine* of the same phase difference.

It is perhaps worth mentioning that the conclusions drawn by Young *et al.*[3] that the ^{12}C(p,γ_0)^{13}N cross section angular distributions in the vicinity of $E_p=1.70$ MeV can be explained entirely in terms of resonant proton capture proceeding through the known states of ^{13}N ($E_x=2.366$ and $E_x=3.512$) and without involving additional background contributions are based on flawed analysis. A more complete discussion of the problems found in Ref. 3 is contained in Ref. 14.

SUMMARY AND CONCLUSIONS

We have applied R-matrix theory to the radiative capture reaction ^{12}C($\vec{p}$,γ)^{13}N in the energy region of the

$E_p = 1.7$ MeV resonance. The collision matrix elements, representing the dynamics of the radiative capture transition, were divided into two contributions according to whether the spatial integration involved the internal or external region. The external region part of a collision matrix element is very nearly model independent being determined by the elastic scattering phase shifts, without the need to introduce an optical potential as one would require if one wanted the small r behavior of the elastic scattering wave function. In contrast, the internal region collision matrix elements are completely dependent on a nuclear model for their evaluation. Here we used the strong interaction form of R-matrix theory where we represent the initial wave function in the internal region entirely in terms of compound nucleus formation.

In addition to the extranuclear, i.e., external (direct capture) background it is possible to include, in standard R-matrix fashion, an internal background contribution. In the present analysis no internal background was necessary to fully account for the data. From this fact one may conclude that an internal direct capture mechanism is not discernable in the ^{12}C(p,γ)^{13}N reaction at low energy.

ACKNOWLEDGMENTS

Two of the authors (T.L.T. and S.L.B.) wish to acknowledge the valuable advice and assistance of T. R. Donoghue and L. J. Dries in the proper use of the Ohio State University polarized ion source. Support for the experimental effort by the National Science Foundation is gratefully acknowledged.

*Present address: U. S. A., ERADCOM, NVEOL, Fort Belvoir, VA 22060.

†Present address: American Oil Co., P.O. Box 3092, Houston, TX 77352.

[1]S. L. Blatt, D. B. Nichols, R. G. Arns, J. D. Goss, and H. J. Hausman, Nucl. Instrum. Methods **61**, 232 (1968).

[2]T. L. Tsin, Ph.D. dissertation, Ohio State University, 1976 (unpublished).

[3]F. C. Young, J. C. Armstrong, and J. B. Marion, Nucl. Phys. **44**, 486 (1963).

[4]C. Rolfs and R. E. Azuma, Nucl. Phys. **A227**, 291 (1974).

[5]T. R. Donoghue, W. S. McEver, H. Paetz gen Schieck, J. C. Volkers, C. E. Busch, Sr. Mary A. Doyle, L. J. Dries, and J. L. Regner, in Proceedings of the Second Symposium on Ion Sources and Formation of Beams, Lawrence Berkeley Laboratory Report LBL-339, 1974, p. IV-8-1.

[6]A. M. Lane and R. G. Thomas, Rev. Mod. Phys. **30**, 257 (1958).

[7]R. G. Seyler and H. R. Weller, Phys. Rev. C **20**, 453 (1979).

[8]R. M. Laszewski and R. J. Holt, At. Data Nucl. Data Tables **19**, 305 (1977).

[9]R. G. Seyler and H. R. Weller, At. Data Nucl. Data Tables **23**, 99 (1979).

[10]H. L. Jackson and A. I. Galonsky, Phys. Rev. **89**, 370 (1953); C. W. Reich, G. C. Phillips, and J. L. Russel, Jr., Phys. Rev. **104**, 143 (1956).

[11]A. M. Lane, Rev. Mod. Phys. **32**, 520 (1960).

[12]S. Cohen and D. Kurath, Nucl. Phys. **A101**, 1 (1967).

[13]R. J. Peterson and J. J. Hamill, Phys. Rev. C **22**, 2282 (1980); K. Koyama, J. Phys. Soc. Jpn. **41**, 1445 (1976); R. R. Sercely, R. J. Peterson, P. A. Smith, and E. R. Flynn, Nucl. Phys. **A324**, 53 (1979); P. W. Chudleigh, C. K. Gowers, and E. G. Muirhead, *ibid.* **A123**, 1033 (1969); G. S. Mutchler, D. Rendic, D. E. Velkley, W. E. Sweeney, Jr., and G. G. Phillips, *ibid.* **A172**, 469 (1971); S. Gangadharan and R. L. Wolke, Phys. Rev. C **1**, 1333 (1970); H. T. Fortune, T. J. Gray, W. Trost, and N. R. Fletcher, Phys. Rev. **179**, 1033 (1969).

[14]J. C. Brown, Ph.D. dissertation, Ohio State University, 1983 (unpublished).